Am J Cancer Res 2024;14(3):1217-1226
www.ajcr.us /ISSN:2156-6976/ajcr0153763

Original Article

Predictive nomogram for bone metastases in lung cancer based on monocyte infiltration

Zhangyan Ke[1,2*], Meiling Zhao[3*], Furong Meng[1,2*], Lulu Zhang[1], Hao Zhang[4], Yajing Ning[1,2], Yingying Zhu[1,2], Xiaoyun Fan[1,2], Yanbei Zhang[1,2]

[1]Department of Geriatric Respiratory and Critical Care Medicine, The First Affiliated Hospital of Anhui Medical University, Hefei, Anhui, China; [2]Anhui Geriatric Institute, The First Affiliated Hospital of Anhui Medical University, Hefei, Anhui, China; [3]Department of Gerontology, Bishan District People's Hospital of Chongqing, Chongqing, China; [4]Fuyang Second People's Hospital, Fuyang, Anhui, China. [*]Equal contributors.

Received October 4, 2023; Accepted February 25, 2024; Epub March 15, 2024; Published March 30, 2024

Abstract: The presence of bone metastases (BM) in patients with lung cancer is indicative of a worse prognosis. The present study aims to investigate the risk factors associated with BM in patients with lung cancer. Patients with lung cancer admitted to the First Affiliated Hospital of Anhui Medical University between June 2019 and September 2021 were enrolled in this study. A nomogram was constructed based on the outcomes derived from univariate and multivariate analyses. Concordance index, calibration plots, receiver operating characteristic curves, and decision curve analysis were used to evaluate the nomogram. To substantiate the influence of monocytes on lung cancer BM, various assays, including cell co-culture, Transwell, wound-healing assays, and immunohistochemistry and immunofluorescence staining, were conducted. Statistical analyses were performed using SPSS 22.0 software and GraphPad Prism 7.0. A total of 462 eligible patients were enrolled, comprising 220 with BM and 242 without. Multivariate analysis revealed that histological type, medical history, monocyte percentage, and LDH (Lactate Dehydrogenase) and ALP (Alkaline Phosphatase) levels were independent risk factors for BM in lung cancer. Transwell and wound-healing assays indicated that co-culture with monocytes significantly enhanced the migration and invasion capabilities of A549 cells in vitro. Immunohistochemistry and immunofluorescence analyses demonstrated a noteworthy increase in monocyte infiltration in the primary lesions of patients with lung cancer with BM. In conclusion, this study successfully constructed and validated a precise, straightforward, and cost-effective prognostic nomogram for patients with lung cancer with BM.

Keywords: Lung cancer, nomogram, bone metastases, monocyte

Introduction

Lung cancer stands as one of the most prevalent malignant tumors globally. According to the latest data on tumor burden from GLOBOCAN2020, the top five cancers in China include lung cancer, colorectal cancer, gastric cancer, breast cancer, and liver cancer. Notably, lung cancer ranks as the leading cause of cancer-related deaths for both men and women [1]. In advanced lung cancer, the skeletal system emerges as the earliest and most common site for metastasis [2]. Skeletal metastases contribute to approximately 350,000 annual fatalities in the United States alone, a figure that nearly triples when considering patients in European countries and Japan [3]. Multiple bone metastases give rise to diverse complications such as pain, hypercalcemia, anemia, heightened infection susceptibility, skeletal fractures, spinal cord compression, spinal instability, and diminished mobility [4]. These complications collectively compromise the functional status and overall quality of life of patients. In addition, they are recognized as risk factors associated with heightened tumor cell activity and malignancy, leading to a poor prognosis [5]. Early intervention strategies have proven effective in mitigating the incidence of complications and associated medical expenses [6]. Therefore, the timely identification of the status of bone metastasis (BM) is of paramount importance.

Previous studies have established correlations between BM and various clinical characteris-

https://doi.org/10.62347/VZLY9631

Table 1. The basic characteristics of enrolled patients with lung cancer

Variables	BM (-, n = 242)	BM (+, n = 220)
Age (y)	66.4 ± 10.2	62.8 ± 10.8
Gender		
Male	163	127
Female	79	93
Histological type		
LUAD	143	172
SCC	63	24
SCLC	36	24
Medical history		
None	111	117
Chronic disease	101	60
Surgery history	30	43
BMI (kg/m^2)	22.3 ± 3.4	21.9 ± 3.2
Monocyte count	0.47 ± 0.21	0.52 ± 2.61
Eosinophil count	0.19 ± 0.22	0.18 ± 0.27
Monocyte (%)	6.9 ± 1.9	7.5 ± 2.9
Eosinophil (%)	2.8 ± 2.7	2.6 ± 2.6
Platelet number	231.4 ± 91.1	231.1 ± 91.2
D-D dimer level	1.3 ± 2.1	2.3 ± 3.5
LDH level	209.2 ± 95.9	253.2 ± 142.5
ALP level	82.6 ± 27.1	134.7 ± 126.1
HSP90a level	90.1 ± 50.5	100.4 ± 59.9

tics. Noteworthy risk factors for BM in patients with lung cancer include lower blood calcium, T4 stage, N3 stage, P-stage III, nonsquamous histology, bone sialoprotein expression, and elevated carcino-embryonic antigen levels [3]. Other studies have delved into bone metabolism, observing increased blood levels of osteopontin, osteocalcin, alkaline phosphatase, phosphorus, lithium, lead, strontium, and cobalt, coupled with a decrease in calcium, magnesium, and manganese in patients with BM [7]. However, limited research has been dedicated to exploring the predictive value of general peripheral blood indices for BM, such as monocyte percentage, D-D dimer level, and LDH levels.

During tumor follow-up, economic considerations and radiation damage prevent the performance of bone scans or magnetic resonance imaging for every session, potentially delaying the detection of partial BM. Hence, an economical and highly sensitive non-invasive predictive model is urgently needed. Therefore, this study aimed to develop a model that accurately predicts the occurrence of BM.

Patients and methods

Population

Peripheral blood indices were collected from 462 patients with lung cancer hospitalized at the First Affiliated Hospital of Anhui Medical University between June 2019 and September 2021. This study was approved by the Ethical Committee of the First Affiliated Hospital of Anhui Medical University. Inclusion criteria comprised patients with a pathological diagnosis of small cell lung cancer or non-small cell lung cancer, along with histopathologically confirmed BM of lung cancer or bone nuclide scans and magnetic resonance imaging suggesting BM. Exclusion criteria encompassed undefined pathological types, multi-tumor status, and the presence of autoimmune diseases affecting bone nuclide scanning.

Data collection

We used serological test results to predict the presence of BM in lung cancer. Consequently, the following details were collected from each enrolled patient: age, gender, histological type, medical history, BMI (kg/m^2), monocyte count, eosinophil count, monocyte percentage, eosinophil percentage, platelet number, D-D dimer level, LDH level, alkaline phosphatase (ALP) level, and heat shock protein 90a (HSP90a) level. Subsequently, all patients were categorized into two groups, namely the BM group (BM+) and the non-BM group (BM-).

Cell culture and co-culture

The lung cancer cell line A549 and monocytes were sourced from GeneChem. All cell lines were cultured in RPMI-1640 medium (Corning, Corning, NY, USA), supplemented with 10% fetal bovine serum (FBS) (Clark Bioscience, Richmond, VA, USA), penicillin (100 U/ml), and streptomycin (100 mg/ml) (HyClone, Logan, UT, USA) in a humidified atmosphere at 37°C with 5% CO_2. For cell co-culture, monocytes were placed in the upper layer of the Transwell chamber, and A549 cells were seeded into the culture plate. After 72 h of co-culture, the Transwell chamber was removed from the culture plate containing A549 cells.

Transwell

A 24-well plate housed the Transwell chamber, where a mixture of diluted matrigel matrix (BD

Table 2. Univariate and multivariate analyses of bone metastasis in lung cancer

Variables	Univariate analysis		Multivariate analysis	
	χ^2 or t value	*P*-value	OR	*P*-value
Age (y)	3.66	<0.001	1.53	0.22
Gender	4.57	0.03	3.19	0.07
Male				
Female				
Histological type	21.51	<0.001	11.62	0.00
LUAD				
SCC				
SCLC				
Medical history	11.82	0.003	9.46	0.01
None				
Chronic disease				
Surgery history				
BMI (kg/m^2)	1.16	0.25	-	-
Monocyte count	2.19	0.02	1.97	0.16
Eosinophil count	0.23	0.81	-	-
Monocyte (%)	2.36	0.01	7.02	0.01
Eosinophil (%)	0.76	0.44	-	-
Platelet number	0.31	0.98	-	-
D-D dimer level	3.64	<0.001	0.01	0.99
LDH level	3.86	<0.002	4.81	0.03
ALP level	6.00	<0.003	37.72	<0.001
HSP90a level	1.32	0.18	-	-

Bioscience, San Jose, CA, USA) and A549 cells in 100 μL of serum-free medium was introduced to the upper chamber. Subsequently, 650 μL of RPMI-1640 medium containing 20% FBS was added to the lower chamber. After incubation for approximately 24 h, the chamber contents were fixed with 4% paraformaldehyde for 20 min and stained with 1% crystal violet for 15 min. Cells on the upper surface of the chamber were removed and observed using a microscope.

Wound-healing assay

For the wound-healing assay, A549 cells were seeded in 6-well plates. The following day, once the cells had adhered to the bottom and achieved 90% confluency, the RPMI-1640 medium was replaced with FBS-free RPMI-1640 after creating linear wounds. The wound closure progress was recorded at 0, 48 h, and 72 h using the Cell discovery7 Live Cell Station.

Immunohistochemistry and immunofluorescence staining

Immunohistochemical (IHC) staining was performed to analyze the expressions of Ki67, following established protocols [8]. Immunofluorescence (IF) staining was conducted to confirm the expressions of CD14, CD16, and CD11c. Tissue slices were blocked with 5% bovine serum albumin at room temperature for 1 h, covered with specific primary antibodies, and incubated at 4°C overnight. The next day, the tissue slices were incubated with a fluorescent secondary antibody (Thermo, USA, 1:250) for 1 h at room temperature. Finally, 4',6-diamidino-2-phenylindole (DAPI) staining was executed for 15 min, and images were recorded using CaseViewer software.

Statistical analysis

Continuous variables were presented as mean ± standard deviation. For univariate analysis, continuous data were assessed using the Student's t-test, while categorical data were analyzed using the chi-square test. For multivariate analysis, logistic regression analysis was used to analyze significant variables in univariate analysis (P<0.05). The nomogram was constructed based on the results of both univariate and multivariate analyses. The predictive performance of the BM prediction model was evaluated using the concordance index. Calibration plots were used to depict the consistency between the nomogram-predicted and actual events. Receiver operating characteristic (ROC) curves were employed to assess the sensitivity and specificity of the nomogram, and decision curve analysis (DCA) was conducted to evaluate the clinical applicability of this model [9].

Results

Patient characteristics

A total of 462 eligible patients were selected, comprising 220 with BM and 242 without. Among the patients, 290 (62.7%) were male, and 315 (68.2%) were diagnosed with adeno-

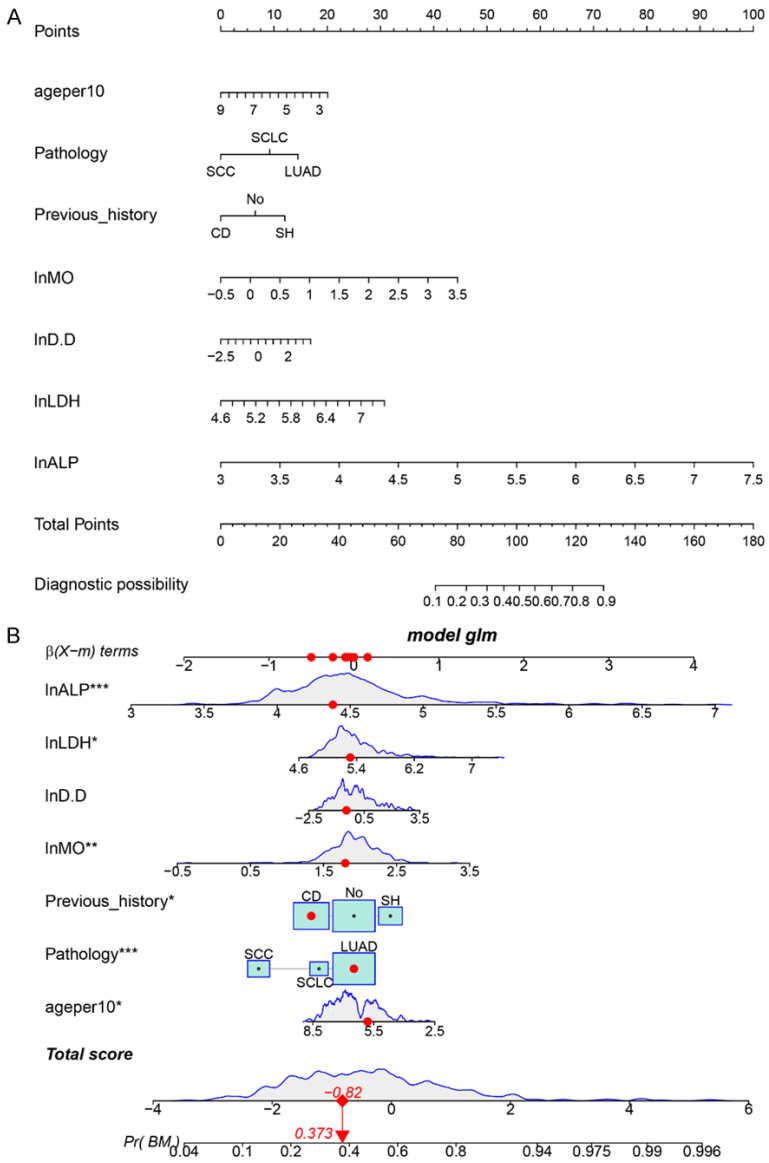

Figure 1. Linear static nomogram and dynamic nomogram depict the entire model and individual patient points, respectively. A: Linear static nomogram; B: Dynamic nomogram.

carcinoma. Medical histories, including chronic diseases and surgical interventions, were also assessed. The findings revealed that 161 (34.8%) patients had concurrent chronic diseases such as hypertension, diabetes, and coronary heart disease, while 73 (15.8%) had undergone prior surgical procedures. Additional patient characteristics are detailed in **Table 1**.

Univariate and multivariate analyses

Patients were divided into the BM+ and BM- groups for subsequent univariate and multivariate analyses. The results of the univariate analyses identified age, gender, histological type, medical history, monocyte count, monocyte percentage, D-D dimer level, LDH level, and ALP level as risk factors for BM in lung cancer. Multivariate analysis pinpointed histological type, medical history, monocyte percentage, LDH level, and ALP level as independent risk factors for BM in lung cancer. These results are shown in **Table 2**.

Construction and validation of a nomogram

Nomograms were constructed based on the outcomes of univariate and multivariate analyses. Both linear static and dynamic nomograms were generated to illustrate the overall points of the model and individual patients, respectively (**Figure 1A**, **1B**). Subsequently, ROC curves, DCA, and calibration plots were used to assess the predictive model (**Figure 2**). The area under the curve (AUC) ROC of the nomogram was 0.777 (**Figure 2A**), indicating high sensitivity and specificity. The calibration plot showed significant consistency between predicted and actual events (**Figure 2B**). The DCA results aligned with those of the ROC and calibration plot (**Figure 2C**). Taken together, these indicators suggest that the constructed nomogram model for BM in lung cancer serves as a highly accurate predictive tool.

Co-culture with monocytes enhances the migration and invasion capacity of A549 cells in vitro

To elucidate the in vitro function of monocytes, A549 cells underwent co-culture with monocytes for 72 h (**Figure 3A**). The initial assess-

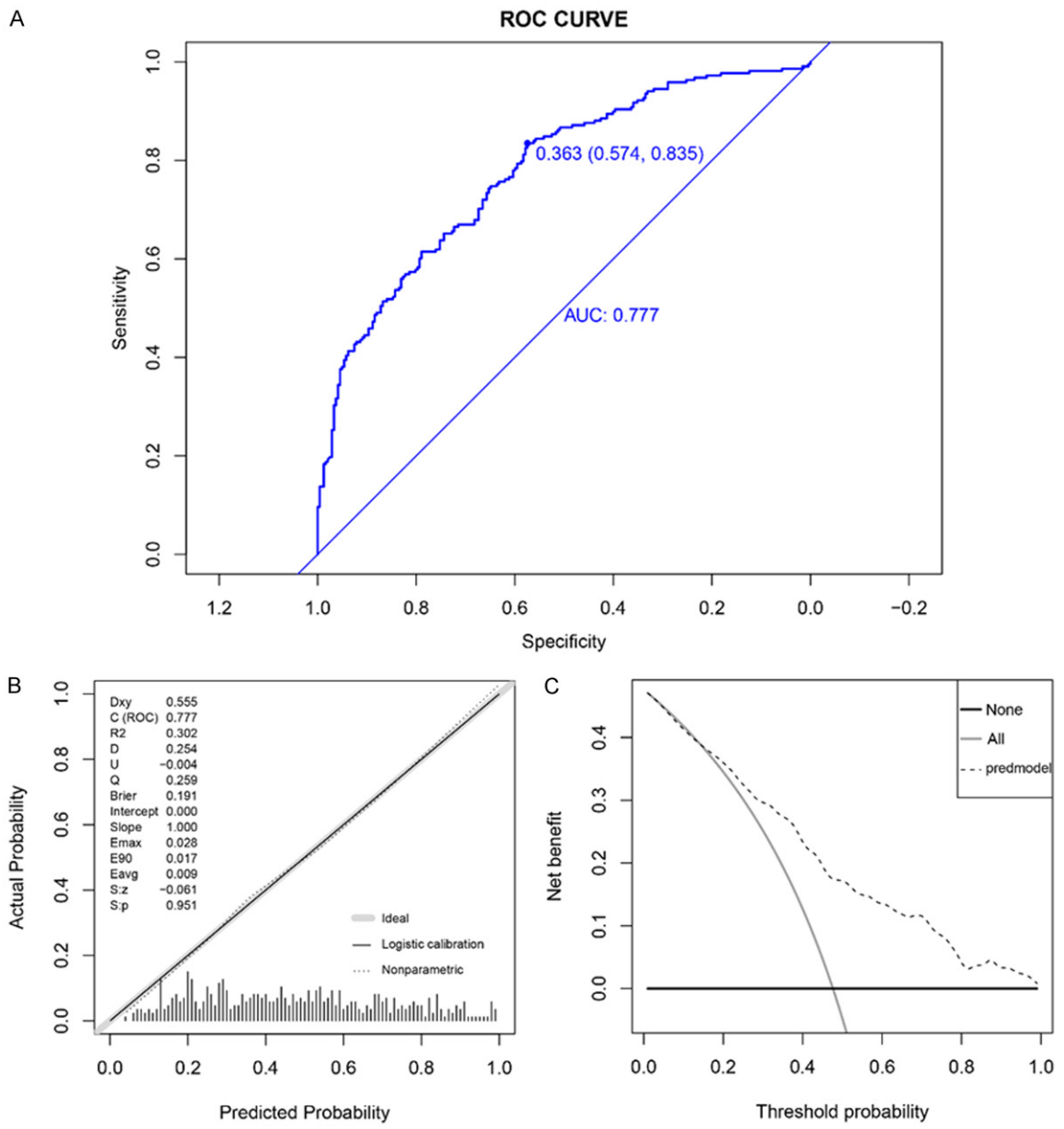

Figure 2. ROC curves, DCA, and calibration plots were used to assess the predictive model. A: AUC of the nomogram was 0.777, indicating high sensitivity and specificity; the optimum cutoff value was 0.363 (0.574, 0.853). B: Calibration plot demonstrates consistency between predicted and actual events. C: DCA yields results consistent with ROC and calibration plot.

ment focused on changes in vertical migration and invasion capacity after co-culture with monocytes, revealing a substantial upregulation in A549 cell vertical migration and invasion capacities (**Figure 3B**, **3C**). Wound-healing assay further demonstrated a marked increase in the horizontal migration capacities of A549 cells upon co-culture with monocytes (**Figure 3D**, **3E**). These findings indicate that co-culturing with monocytes promotes the migration and invasion capacity of A549 cells in vitro.

Increased monocyte infiltration in the primary lesions of lung cancer with bone metastasis

To verify the preceding results, 10 patients with or without lung cancer BM were selected. IHC for Ki67 was employed to assess the proliferative activity of the selected lesions. The outcomes indicated increased Ki67 levels in patients in the BM+ group compared to those in the BM- group, as shown in **Figure 4A-D**. To investigate monocyte infiltration in patients

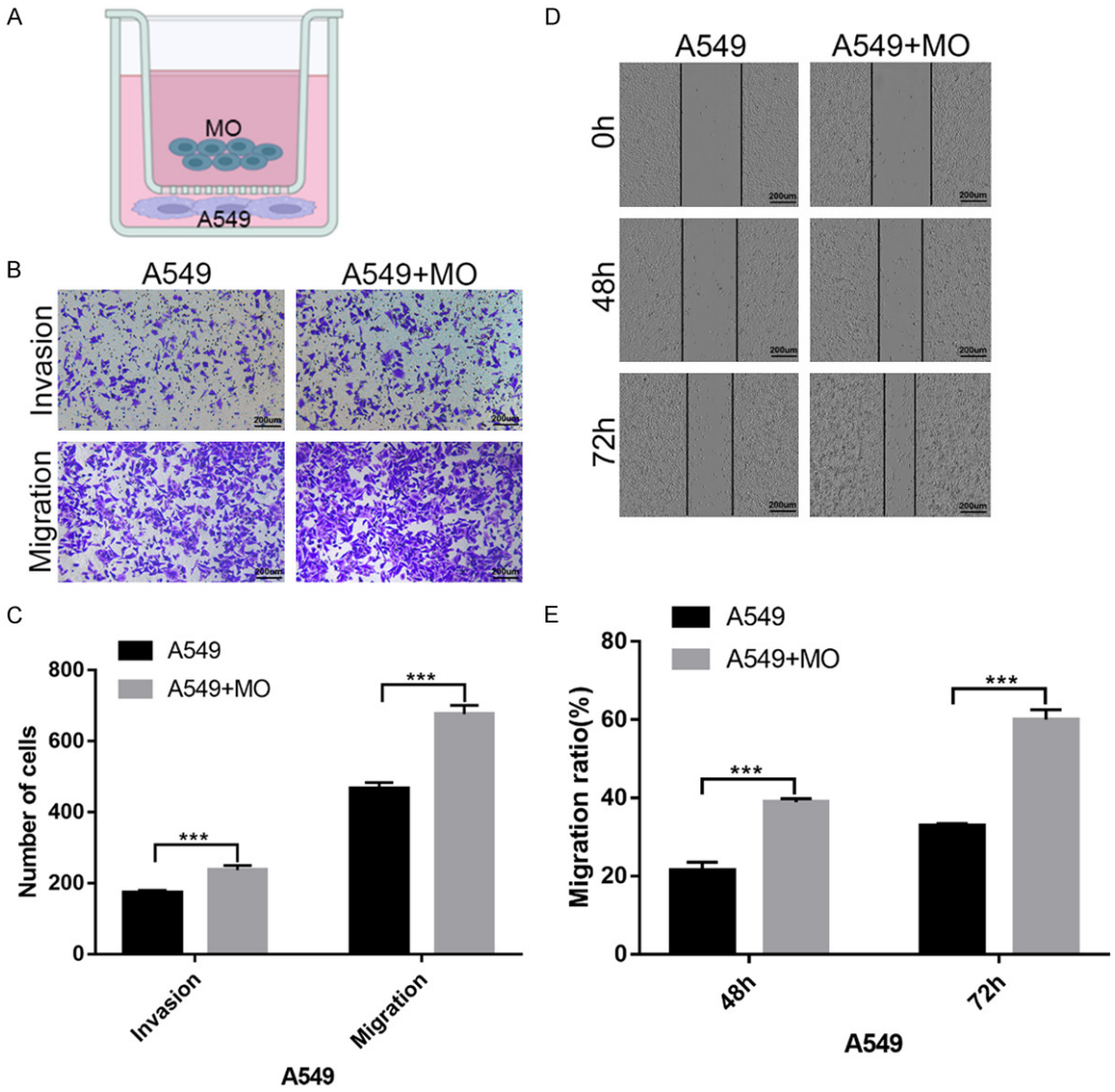

Figure 3. Co-culture with monocytes enhances A549 cell migration and invasion capacity in vitro. A: A549 cells co-cultured with monocytes for 72 h; B, C: Transwell assay reveals significantly increased vertical migration and invasion capacities upon co-culture with monocytes; D, E: Wound-healing assay shows enhanced horizontal migration capacities upon co-culture with monocytes.

with lung cancer with BM, IF for monocyte immune markers, such as CD11C, CD16, and CD14, was conducted. These findings demonstrated a significant increase in monocyte infiltration within the primary lesions of patients with lung cancer with BM (**Figure 5A**, **5B**).

Discussion

The bone serves as a predominant site for hematogenous metastasis in lung cancer, with its occurrence signaling a decline in the patient's quality of life and a shortened survival period. Previous studies estimate the incidence of BM in lung cancer to be approximately 10%-15% [10]. Patients experiencing BM witness a significant reduction in quality of life and a median survival time ranging from 6 to 10 months, with a one-year survival rate post-treatment around 40% to 50% [11]. Skeletal-related events afflict 46% of patients with BM, significantly shortening their survival time [12]. Early detection and treatment become imperative for patients with lung cancer and BM, emphasizing the critical need for predictive models. While recent studies on BM in lung

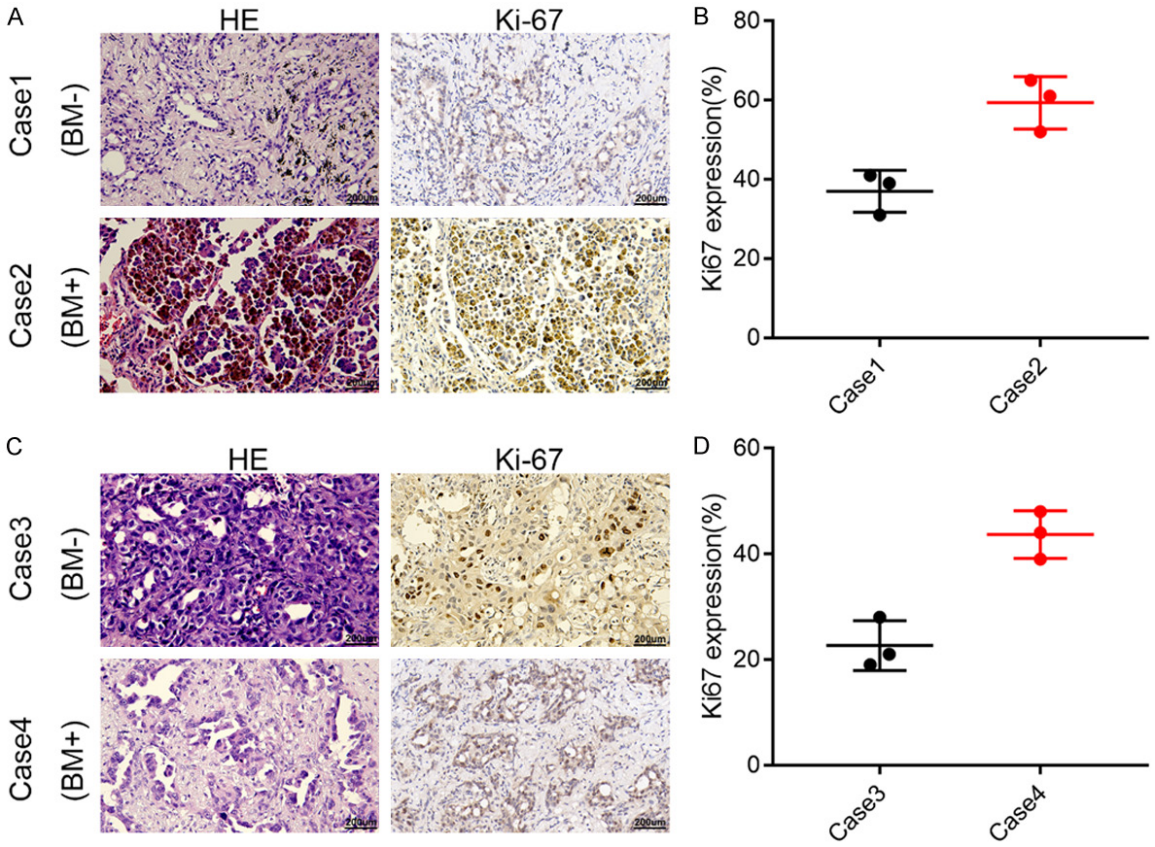

Figure 4. The representative IHC pictures for Ki67 indicate increased levels in BM+ group compared to those in BM- group. A, B: The representative images and immunohistochemical scores of Case1-2. C, D: The representative images and immunohistochemical scores of Case3-4.

cancer have predominantly operated at the molecular level [13, 14], our study focuses on clinical data accessibility. We analyzed 462 lung cancer patients, categorizing them into the BM+ and BM- groups, employing the latest clinical diagnosis and treatment expert consensus on BM in lung malignancies. Through univariate and multivariate regression analyses of clinical basic information and peripheral blood indicators, an economical and simple predictive model for lung cancer BM was successfully established, presenting a promising clinical application value.

Univariate analysis revealed that patients in the BM+ group at the time of their initial diagnosis were younger than those in the BM- group, potentially linked to higher metabolic levels in younger individuals. Specific mechanisms underlying this association, such as slower cell proliferation [15], altered concentration of hormones and cell responsiveness to hormones [16], and impaired angiogenesis [17], have been previously reported. Gender analysis indicated that female patients were more prone to BM, though not independently significant, implying the influence of other factors on BM occurrence in females. Further analyses identified histological type, particularly adenocarcinoma, as an independent risk factor for lung cancer metastasis, aligning with the higher prevalence of adenocarcinoma in females [18]. Subsequent analysis of peripheral blood indicators, such as monocyte count and percentage, eosinophil count and percentage, platelet level, D-D dimer level, LDH level, ALP level, and Hsp90α level, was performed, identifying monocyte percentage, LDH level, and ALP level as independent risk factors for lung cancer BM. Elevated LDH reflects tumor burden [19], predicting BM status in digestive system tumors [20]. High ALP levels are recognized as independent risk factors in various solid tumors [21-25]. In addition, the present study found a higher monocyte percentage in the BM+ group than the BM- group, a novel

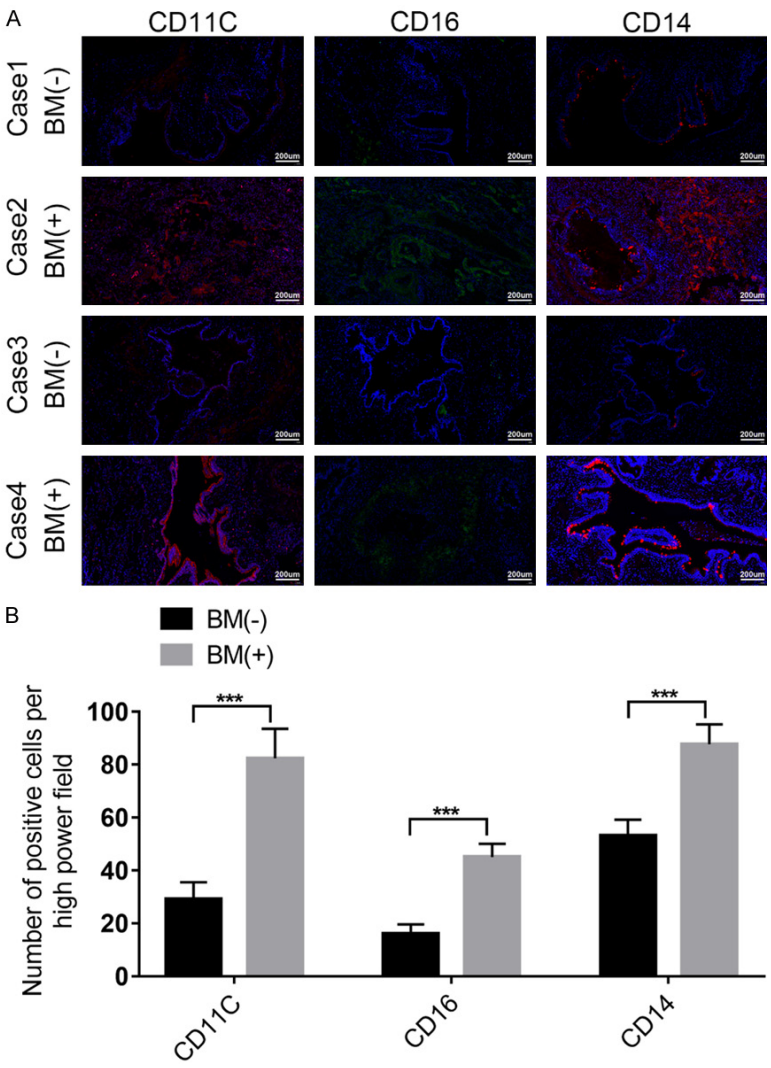

Figure 5. IF for CD11C, CD16, and CD14 demonstrates significantly increased monocyte infiltration in the primary lesions of patients with lung cancer with BM. A: The representative images of CD11C, CD16, and CD14 in Case1-4. B: The fluorescence intensity evaluation of CD11C, CD16, and CD14 in Case1-4.

observation in lung cancer BM. However, relevant studies have confirmed that breast cancer cells secrete diverse cytokines, promoting monocyte chemotaxis within the bone tissue. This phenomenon establishes a microenvironment suitable for tumor cell metastasis, effectively facilitating the metastatic process [26, 27]. We posit that a similar mechanistic pathway may be plausible in lung cancer BM.

The univariate analysis revealed that age, pathological type, medical history, monocyte count and percentage, D-D dimer, LDH level, and ALP level were risk factors for lung cancer BM. Subsequently, indicators with statistical significance in the univariate analysis were incorporated into the multivariate analysis. The findings identified pathological type, medical history, monocyte percentage, LDH level, and ALP level as independent risk factors for lung cancer BM. Summarizing these independent risk factors, we constructed a prediction model for lung cancer BM. The prediction model with an AUC ROC curve of 0.777 exhibited high sensitivity and specificity. Consistency testing and internal verification revealed significant alignment between predicted and actual values, highlighting its strong clinical application value. Similar results were observed in the DCA curve and consistency test, affirming the robust forecasting accuracy and practical utility of our multifactorial analysis-derived model. The fundamental experiments, including cell co-culture, Transwell, wound-healing assay, and immunohistochemistry and immunofluorescence staining, demonstrated the promotion of lung cancer BM by monocyte infiltration.

However, this study has certain limitations. First, the lack of comprehensive research data introduces selection bias. Second, the single-center study raises concerns about generalizability due to the predominance of patients with advanced stages of complex conditions, potentially contributing to bias. Lastly, certain unexplained results, such as the post-surgery propensity for BM, warrant further clarification through large-scale sample studies.

Conclusion

This study constructed a predictive model for lung cancer bone metastasis by analyzing accessible and predictive indicators, demonstrating high clinical application value. However,

subsequent studies are needed for further confirmation.

Disclosure of conflict of interest

None.

Address correspondence to: Yanbei Zhang and Xiaoyun Fan, Department of Geriatric Respiratory and Critical Care Medicine, The First Affiliated Hospital of Anhui Medical University, Hefei, Anhui, China. E-mail: zhangyanbei1963@126.com (YBZ); 13956988552@126.com (XYF)

References

[1] Cao W, Chen HD, Yu YW, Li N and Chen WQ. Changing profiles of cancer burden worldwide and in China: a secondary analysis of the global cancer statistics 2020. Chin Med J (Engl) 2021; 134: 783-791.

[2] Zhang L and Gong Z. Clinical characteristics and prognostic factors in bone metastases from lung cancer. Med Sci Monit 2017; 23: 4087-4094.

[3] Niu Y, Lin Y, Pang H, Shen W, Liu L and Zhang H. Risk factors for bone metastasis in patients with primary lung cancer: a systematic review. Medicine (Baltimore) 2019; 98: e14084.

[4] Jimenez-Andrade JM, Mantyh WG, Bloom AP, Ferng AS, Geffre CP and Mantyh PW. Bone cancer pain. Ann N Y Acad Sci 2010; 1198: 173-181.

[5] Selvaggi G and Scagliotti GV. Management of bone metastases in cancer: a review. Crit Rev Oncol Hematol 2005; 56: 365-378.

[6] Delea T, Langer C, McKiernan J, Liss M, Edelsberg J, Brandman J, Sung J, Raut M and Oster G. The cost of treatment of skeletal-related events in patients with bone metastases from lung cancer. Oncology 2004; 67: 390-396.

[7] Dumanskiy YV, Syniachenko OV, Stepko PA, Taktashov GS, Chernyshova OY and Stoliarova OY. The state of bone metabolism in lung cancer patients. Exp Oncol 2018; 40: 136-139.

[8] Wang M, Li J, Yang X, Yan Q, Wang H, Xu X, Lu Y, Li D, Wang Y, Sun R, Zhang S, Zhang Y, Zhang Z, Meng F and Li Y. Targeting TLK2 inhibits the progression of gastric cancer by reprogramming amino acid metabolism through the mTOR/ASNS axis. Cancer Gene Ther 2023; 30: 1485-1497.

[9] Vickers AJ and Elkin EB. Decision curve analysis: a novel method for evaluating prediction models. Med Decis Making 2006; 26: 565-574.

[10] Hernandez RK, Wade SW, Reich A, Pirolli M, Liede A and Lyman GH. Incidence of bone metastases in patients with solid tumors: analysis of oncology electronic medical records in the United States. BMC Cancer 2018; 18: 44.

[11] Nistor CE, Ciuche A, Cucu AP, Nitipir C, Slavu C, Serban B, Cursaru A, Cretu B and Cirstoiu C. Management of lung cancer presenting with solitary bone metastasis. Medicina (Kaunas) 2022; 58: 1463.

[12] Yonezawa N, Murakami H, Sangsin A, Mizukoshi E and Tsuchiya H. Lung metastases regression with increased CD8+ T lymphocyte infiltration following preoperative spinal embolization and total en bloc spondylectomy using tumor-bearing frozen autograft in a patient with spinal metastatic leiomyosarcoma. Eur Spine J 2019; 28: 41-50.

[13] Ren G, Esposito M and Kang Y. Bone metastasis and the metastatic niche. J Mol Med (Berl) 2015; 93: 1203-1212.

[14] Wang L, Song L, Li J, Wang Y, Yang C, Kou X, Xiao B, Zhang W, Li L, Liu S and Wang J. Bone sialoprotein-αvβ3 integrin axis promotes breast cancer metastasis to the bone. Cancer Sci 2019; 110: 3157-3172.

[15] Holbrook NJ and Ikeyama S. Age-related decline in cellular response to oxidative stress: links to growth factor signaling pathways with common defects. Biochem Pharmacol 2002; 64: 999-1005.

[16] Roth GS. Hormone action during aging: alterations and mechanisms. Mech Ageing Dev 1979; 9: 497-514.

[17] Reed MJ and Edelberg JM. Impaired angiogenesis in the aged. Sci Aging Knowledge Environ 2004; 2004: pe7.

[18] Riihimäki M, Hemminki A, Fallah M, Thomsen H, Sundquist K, Sundquist J and Hemminki K. Metastatic sites and survival in lung cancer. Lung Cancer 2014; 86: 78-84.

[19] Peng L, Wang Y, Liu F, Qiu X, Zhang X, Fang C, Qian X and Li Y. Peripheral blood markers predictive of outcome and immune-related adverse events in advanced non-small cell lung cancer treated with PD-1 inhibitors. Cancer Immunol Immunother 2020; 69: 1813-1822.

[20] Ma X, Fan Y, Chen Z, Zhang Y, Wang S and Yu J. Blood biomarkers of bone metastasis in digestive tract malignant tumors. Future Oncol 2021; 17: 1507-1518.

[21] Wang N, Liu F, Xi W, Jiang J, Xu Y, Guan B, Wu J, Zhou C, Shi M, Zhu Z, Xu Y, Liu J and Zhang J. Development and validation of risk and prognostic nomograms for bone metastases in Chinese advanced colorectal cancer patients. Ann Transl Med 2021; 9: 875.

[22] Hammerich KH, Donahue TF, Rosner IL, Cullen J, Kuo HC, Hurwitz L, Chen Y, Bernstein M, Coleman J, Danila DC and Metwalli AR. Alkaline phosphatase velocity predicts overall survival and bone metastasis in patients with castra-

tion-resistant prostate cancer. Urol Oncol 2017; 35: 460.e21-460.e28.
[23] Jiang C, Hu F, Xia X and Guo X. Prognostic value of alkaline phosphatase and bone-specific alkaline phosphatase in breast cancer: a systematic review and meta-analysis. Int J Biol Markers 2023; 38: 25-36.
[24] Lim SM, Kim YN, Park KH, Kang B, Chon HJ, Kim C, Kim JH and Rha SY. Bone alkaline phosphatase as a surrogate marker of bone metastasis in gastric cancer patients. BMC Cancer 2016; 16: 385.
[25] Du WX, Duan SF, Chen JJ, Huang JF, Yin LM and Tong PJ. Serum bone-specific alkaline phosphatase as a biomarker for osseous metastases in patients with malignant carcinomas: a systematic review and meta-analysis. J Cancer Res Ther 2014; 10: C140-C143.
[26] Jiang P, Gao W, Ma T, Wang R, Piao Y, Dong X, Wang P, Zhang X, Liu Y, Su W, Xiang R, Zhang J and Li N. CD137 promotes bone metastasis of breast cancer by enhancing the migration and osteoclast differentiation of monocytes/macrophages. Theranostics 2019; 9: 2950-2966.
[27] Magidey-Klein K, Cooper TJ, Kveler K, Normand R, Zhang T, Timaner M, Raviv Z, James BP, Gazit R, Ronai ZA, Shen-Orr S and Shaked Y. IL-6 contributes to metastatic switch via the differentiation of monocytic-dendritic progenitors into prometastatic immune cells. J Immunother Cancer 2021; 9: e002856.